Decay rates of charmonia within a quark-antiquark confining potential *

Smruti Patel[1;1)], P. C. Vinodkumar[1;2)], Shashank Bhatnagar[2;3)]

[1] Department of Physics, Sardar Patel University,Vallabh Vidyanagar, India
[2] Department of Physics, Addis Ababa University, P.O.Box 101739, Addis Ababa, Ethiopia

Abstract: In this work, we investigate the spectroscopy and decay rates of charmonia within the framework of the non-relativistic Schrödinger equation by employing an approximate inter quark-antiquark potential. The spin hyperfine, spin-orbit and tensor components of the one gluon exchange interaction are employed to compute the spectroscopy of the excited S states and a few low-lying P and D waves. The resultant wave functions at zero inter-quark separation as well as some finite separations are employed to predict the di-gamma, di-leptonic and di-gluon decay rates of charmonia states using the conventional Van Royen-Weisskopf formula. The di-gamma and di-leptonic decay widths are also computed by incorporating the relativistic corrections of order v^4 within the NRQCD formalism. We have observed that the NRQCD predictions with their matrix elements computed at finite radial separation yield results which are found to be in better agreement with experimental values for both di-gamma and di-leptonic decays. The same scenario is seen in the case when di-gamma and di-leptonic decay widths are computed with the Van Royen-Weisskopf formula. It is also observed that the di-gluon decay width with the inclusion of binding energy effects are in better agreement with the experimental data available for $1S$-$2S$ and $1P$. The di-gluon decay width of $3S$ and $2P$ waves waves are also predicted. Thus, the present study of decay rates clearly indicates the importance of binding energy effects.

Keywords: potential models, heavy quarkonia, radiative decays, non relativistic quark model

PACS: 12.39.Pn; 14.40.Pq; 13.20.Gd **DOI:** 10.1088/1674-1137/40/5/053102

1 Introduction

After a hiatus of about three decades, charmonium has proved a remarkable laboratory for the study of quantum chromodynamics (QCD). Following a period of several years of intense experimental activity, charmonium physics has emerged again as one of the most exciting areas of experimental high energy physics due to the massive dedicated investigations by experimenters. The large quantity of new data coming from different experimental groups like BaBar, CLEO, SELEX, Tevatron and other B factories the world over as well as the progress made in theoretical methods in the last few years has greatly changed the thrust in this area [1–3]. The study of quarkonium spectra provides fundamental informations about the interquark potential. Yet, despite the apparent simplicity of these states, the mechanism behind their production remains a mystery, even after decades of experimental and theoretical efforts [4]. The production rate in various high energy processes can give valuable insight into the heavy quark-antiquark interactions as well as into the elementary processes leading to the production of the $c\bar{c}$ pair. Furthermore, these mesons enter a number of reactions which are of greatest importance for the study of the Cabibbo-Kobayashi-Maskawa (CKM) matrix and of CP violation.

The spectroscopy and decay rates of quarkonia are quite important to study as the huge amount of high precision data acquired from many experimental facilities world over is continuously providing more accurate information about hadrons, particularly in the charm and beauty flavour sectors [5, 6]. Many theoretical predictions on the decay properties, particularly the leptonic and di-gamma decays of quarkonia, based on the relativistic quark model or potential model [7–9], Bethe-Salpeter equation [10, 11], heavy-quark spin symmetry [12] and lattice QCD [13] are available in the literature. The spectroscopic parameters like the inter-quark poten-

Received 13 August 2015, Revised 12 November 2015
∗ Supported by Major Research Project NO. F. 40-457/2011(SR), UGC, India
1) E-mail: fizixsmriti31@gmail.com
2) E-mail: p.c.vinodkumar@gmail.com
3) E-mail: shashank-bhatnagar@yahoo.com

tial and its parameters, which describe the masses of the low lying bound states and the resulting wave functions, are important and decisive in the descriptions of other properties like the decay (in the annihilation channel) and transition rates. In this study, we deduce the basic parameters of the mesonic states by fitting the masses of the low lying $c\bar{c}$ states based on a phenomenological potential framework.

The success of any theoretical model for mesons depends on the correct prediction of their decay rates apart from their mass spectra. In many phenomenological models the predictions of the masses are correct but predictions for the decay rates are overestimated [14–18]. The incorporation of various corrections due to radiative processes, higher-order QCD contributions etc. to decay rates have been suggested for better estimates of their decay properties with reference to the experimental data. In this context, the NRQCD formalism is found to provide a systematic treatment of the perturbative and non-perturbative components of QCD at the hadronic scale [19–22]. For this study, we employ phenomenological potential schemes for the bound states of heavy quarkonia and the resulting parameters and wave functions to study the decay properties. The study of di-gamma and di-lepton decay widths of charmonia has been done using the conventional Van Royen Weisskopf formula as well as using the NRQCD formalism.

The paper is organized as follows. In Section 2, we describe the phenomenological quark-antiquark interaction potential and extract the parameters that describe the ground state masses of $c\bar{c}$ system. We also compute the low lying orbital excited states of these systems. In Section 3 we employ the spectroscopic parameters of the $c\bar{c}$ system to study the two-photon and di-leptonic decay widths in conventional as well as NRQCD formalism. In Section 4 we present and analyze our results to draw important conclusions.

2 Phenomenology and extraction of the spectroscopic parameters

There are many methods to estimate the mass of a hadron, among which the phenomenological potential model is a fairly reliable one, especially for heavy hadrons. For the description of the quarkonium bound states, we adopt the phenomenological potential of the form which is expressed in terms of a vector (Coulomb) plus a scalar (confining) part given by

$$V(r)=V_{\rm V}+V_{\rm S}=\frac{-4\alpha_{\rm s}}{3r}+\frac{Ar^2}{(1+4Br^n)^{\frac{1}{2}}}-V_0. \quad (1)$$

Here, $A=0.374$ GeV^3, $B=1.0$ GeV^n, n=1 and $V_{\rm s}$ is a state dependent constant potential. Here, $\alpha_{\rm s}$ is the running strong coupling constant, which is computed as

$$\alpha_{\rm s}(\mu^2)=\frac{4\pi}{\left(11-\frac{2}{3}n_{\rm f}\right)\left(\ln\frac{\mu^2}{\Lambda^2}\right)}, \quad (2)$$

where Λ is the QCD scale, which is taken as 0.120 GeV, $n_{\rm f}$ is the number of flavors and μ is the renormalization scale related to the constituent quark mass. A similar type of potential has been used by Refs. [23–29] with $n=2$ for the study mainly of ground state light flavor hadrons using the field theoretical framework of the Bethe-Salpeter equation under the Covariant Instantaneous Ansatz (CIA), which is a Lorentz-invariant generalization of the Instantaneous Ansatz (IA). Such a type of potential in the above framework was employed for calculations [25, 26, 30] dealing with studies on the leptonic decay constants of ground state vector mesons (ρ, ϕ, ω, ψ, Y) as well as ground state pseudoscalar mesons (π, K, D, D_s, B), two-photon decay widths for the process, $P\rightarrow\gamma\gamma$ and radiative decay widths of light vector mesons through the process $V\rightarrow P\gamma$. In all these studies the confining term in the potential in Eq. (1) is supposed to simulate an effect of an almost linear confinement (r) for the heavy quark (c, b) sector, while retaining the harmonic form of the (r^2) for the light quark (u,d) sector as is believed to be true for QCD.

The use of this potential with index $n=2$ in our numerical approach is found to be inconsistent in correctly predicting the hyperfine splitting between pseudoscalar and vector mesons, even for the ground state. Besides, for orbital excited states the potential behavior becomes repulsive with the use of the r^2 term in the denominator. So we have attempted this potential with index n=1. With the choice of $n=1$ in Eq. (1), the overall shape of the potential (see inserted figure at right bottom corner of Fig. 1) is not altered much and better consistency is found for the predictions of hyperfine and fine structure splitting of the $c\bar{c}$ states. Moreover, the potential with power $n=1$ is shallower than the potential with $n=2$ and this shallow nature is required for the excited state predictions of heavy quarkonia.

We now present the details of our calculations by using the potential with $n=1$ of Eq. (1). Different degenerate $n^{2S+1}L_J$ low-lying states of $c\bar{c}$ mesons are calculated by including the spin dependent part of the usual one-gluon exchange potential [18, 31–34]. The potential description extended to spin dependent interactions results in three types of potential terms such as the spin-spin, the spin-orbit and the tensor part that are to be added to the spin independent potential as given by Eq. (1). Accordingly, the spin-dependent part $V_{\rm SD}$ is given by

$$V_{\rm SD}=V_{\rm SS}\left[\frac{1}{2}\left(S(S+1)-\frac{3}{2}\right)\right]$$

$$+V_{\rm LS}\left[\frac{1}{2}(J(J+1)-S(S+1)-L(L+1))\right]$$
$$+V_{\rm T}\left[12\left(\frac{(S_1.r)(S_2.r)}{r^2}-\frac{1}{3}(S_1.S_2)\right)\right]. \quad (3)$$

The spin-orbit term containing $V_{\rm LS}$ and tensor term containing $V_{\rm T}$ describe the fine structure of the states, while the spin-spin term containing $V_{\rm SS}$ proportional to $2S_1.S_2$ gives the hyperfine splitting. The co-efficient of these spin-dependent terms of Eq. (10) can be written in terms of the vector and scalar parts of static potential V(r)as

$$V^{ij}_{\rm LS}(r)=\frac{1}{2M_iM_jr}\left[3\frac{{\rm d}V_{\rm V}}{{\rm d}r}-\frac{{\rm d}V_{\rm S}}{{\rm d}r}\right], \quad (4)$$

$$V^{ij}_{\rm T}(r)=\frac{1}{6M_iM_j}\left[3\frac{{\rm d}^2V_{\rm V}}{{\rm d}r^2}-\frac{1}{r}\frac{{\rm d}V_{\rm S}}{{\rm d}r}\right], \quad (5)$$

$$V^{ij}_{\rm SS}(r)=\frac{1}{3M_iM_j}\nabla^2V_{\rm V}=\frac{16\pi\alpha_s}{9M_iM_j}\delta^3(r), \quad (6)$$

where M_i, M_j corresponds to the quark masses. The Schrödinger equation with the potential given by Eq.(1) is numerically solved using the Mathematica notebook with the Runge-Kutta method [35] to obtain the energy eigenvalues and the corresponding wave functions.

The computed masses of the nS, nP and nD states are listed in Tables 1, 2 and 3 respectively. The optimized spectroscopic parameters thus correspond to the fitted quark masses, the potential strength V_0 and the corresponding radial wave functions. The quark mass m_c = 1.28 GeV, while the potential strength (V_0) is given by the relation

$$V_0(n+1,l)=V_0(n)+0.02l(3l+5)+\frac{1}{2}, \quad (7)$$

Table 1. Charmonium mass spectra for nS states in GeV.

state	present	[53]	[6]	[54]	[40]	[31]	[55]	[56]
1^3S_1	3.096	3.175	3.097	3.168	3.090	3.090	3.085 ± 0.001	3.097
1^1S_0	2.979	2.966	2.980	3.088	2.976	2.982	3.010 ± 0.001	2.980
2^3S_1	3.680	3.705	3.686	3.707	3.615	3.672	3.739 ± 0.046	3.687
2^1S_0	3.600	3.560	3.638	3.669	3.533	3.630	3.770 ± 0.040	3.631
3^3S_1	4.077	4.106	4.040	4.094	3.962	4.072	–	4.030
3^1S_0	4.011	3.978	–	4.067	3.895	4.063	–	3.992
4^3S_1	4.454	4.442	4.415	4.420	4.240	4.406	–	4.273
4^1S_0	4.397	4.324	–	4.398	4.180	4.384	–	4.244

[6]-Exp
[53, 55]-Lattice
[54]-NRQM
[31, 40, 56]-Potential models

Table 2. Charmonia spectra for $nP(L=1,2)$ waves in GeV.

state	Mcw	$n^{2S+1}L_J$	$V_{\rm T}$ contribution	V_{LS} contribution	present	Exp.[6]	[53]	[54]	[40]	[31]	[55]
$1P$	3.539	1^3P_2	−0.000006	0.025	3.565	3.556	3.491	3.564	3.524	3.556	3.503 ± 0.024
		1^3P_1	0.00003	−0.025	3.514	3.510	3.490	3.520	3.514	3.505	3.472 ± 0.009
		1^3P_0	−0.00006	−0.05	3.488	3.414	3.442	3.448	3.466	3.424	3.408 ± 0.002
		1^1P_1			3.539	3.526	3.486	3.536	3.514	3.516	3.474 ± 0.010
$2P$	3.996	2^3P_2	−0.000004	0.0247	4.021	3.929	3.924	–	–	–	4.030 ± 0.180
		2^3P_1	0.000018	−0.0247	3.972	–	3.917	–	–	–	4.067 ± 0.105
		2^3P_0	−0.000037	−0.0495	3.947	–	3.870	–	–	–	4.008 ± 0.122
		2^1P_1	–	–	3.996	–	3.916	–	–	–	4.053 ± 0.095

Table 3. Charmonia spectra for $nD(n=1,2)$ waves in GeV.

state	Mcw	$n^{2S+1}L_J$	$V_{\rm T}$ contribution	V_{LS} contribution	present	Exp.[6]	[53]	[54]	[40]	[31]
$1D$	3.796	1^3D_3	0.0023	−0.000008	3.798		3.770	3.809	3.83	4.167
		1^3D_2	−0.0011	0.00003	3.794		3.792	3.804	3.854	4.158
		1^3D_1	−0.0034	−0.00003	3.792	3.770	3.796	3.789	3.860	4.142
		1^1D_2			3.796		3.782	3.803	3.844	4.158
$2D$	4.224	2^3D_3	0.0012	−0.000003	4.425					
		2^3D_2	−0.0006	0.00001	4.223					
		2^3D_1	−0.0019	−0.00001	4.222	4.160				
		2^1D_2			4.224					

where l is the orbital angular momentum. The value of $V_0(n=0;l=0)$ is fixed as 0.12 Gev. We have plotted the behaviour of the present potential for different states as shown in Fig. 1.

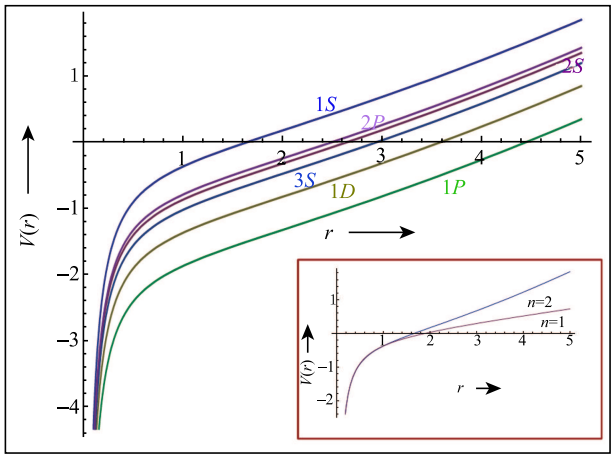

Fig. 1. (color online) Behaviour of the potential different states.

3 Decay rates of heavy quarkonia

Apart from the masses of the low lying mesonic states, the correct predictions of the decay rates are important features of any successful model. There have been a number of recent studies on processes involving strong decays, radiative decays and leptonic decays of vector mesons. Such studies offer a direct probe of hadron structure and help in revealing some aspects of the underlying quark-gluon dynamics that are complementary to what is learnt from pseudoscalar mesons. Leptonic decay constants are simple probes of the short distance structure of hadrons and therefore are a useful observable for testing quark dynamics in this regime. The extracted model parameters and the radial wave functions are employed here to compute the di-leptonic, two-photon and two-gluon annihilation rates and since this rate is related to the wave function, it provides a better understanding of the quark-antiquark dynamics within the meson. This can be a crucial test of a potential model. The radiative decays of the bound $c\bar{c}$ states provide an excellent laboratory for studying charmonium decay dynamics and light hadron spectroscopy. An electromagnetic decay occurs when the $c\bar{c}$ pair annihilates into one or more photons, which can subsequently lead to a pair of leptons as the final state. These processes can be calculated with perturbative quantum electrodynamics (QED) with corrections from the strong interaction.

3.1 Using the Van Royen-Weisskopf formula

A decay to a pair of leptons is only allowed to the states with the same quantum numbers as the photon, that is $J^{PC}=1^{--}$. Using the Van Royen-Weisskopf formula the leptonic decay width with radiative correction for the vector mesons reads:

$$\Gamma(n^3S_1 \longrightarrow l^+l^-) = \frac{4N_c\alpha^2 {e_Q}^2 |R_{nl}(r)|^2}{{M_V}^2}\left[1-\frac{16}{3}\left(\frac{\alpha_S}{\pi}\right)\right], \tag{8}$$

A decay into two photons is instead forbidden to the $J=1$ states by the Yang theorem [36, 37]. For other resonances, the conservation of charge parity requires the S wave states to be in a spin-singlet state and the P-wave states to be in a spin-triplet state. For the S wave digamma decay widths, most of the model predictions are consistent with experimental results, while in the case of P waves the theoretical predictions for digamma widths differs from the experimental results. This discrepancy is somehow removed with the inclusion of QCD corrections. The di-gamma decay widths for the η_Q, χ_{Qo}, χ_{Q2} into two photons with one loop radiative corrections are computed using the non-relativistic expression given by [17, 38–44]

$$\Gamma(n^1S_0 \longrightarrow \gamma\gamma) = \frac{3}{2}\frac{\alpha^2 {e_Q}^4 M_{\eta_Q}|R_{nl}(r)|^2}{{M_Q}^3}\times \left[1-\frac{(20-\pi^2)}{3}\left(\frac{\alpha_S}{\pi}\right)\right], \tag{9}$$

$$\Gamma(n^3P_0 \longrightarrow \gamma\gamma) = \frac{27\alpha^2 {e_Q}^4 M_{\chi_{Q0}}|R^{(l)}_{nl}(r)|^2}{2{M_Q}^3}\times \left[1+\frac{(\pi^3)}{3}\frac{28}{9}\left(\frac{\alpha_S}{\pi}\right)\right], \tag{10}$$

$$\Gamma(n^3P_2 \longrightarrow \gamma\gamma) = \frac{4}{15}\frac{27\alpha^2 {e_Q}^4 M_{\chi_{Q2}}|R^{(l)}_{nl}(r)|^2}{2{M_Q}^3}\times \left[1-\frac{16}{3}\left(\frac{\alpha_S}{\pi}\right)\right]. \tag{11}$$

Among hadronic decays, we can consider annihilations and transitions. The first type of decay occurs when the $c\bar{c}$ pair annihilates into two or more gluons or light quarks. In analogy to the electromagnetic decays, a decay into two gluons gg is allowed to the same states which they can decay into, with respect to which it is much more favoured due to the larger coupling constant. The di-gluon decay width gives information on the total width of the corresponding quarkonium [45].

The relevant theoretical expressions for the di-gluon decay widths of n^1S_0, n^3P_0 and n^3P_2 charmonia states, incorporating the leading order QCD corrections, are given by [38, 46–48]

$$\Gamma_{gg}(\eta_Q) = \frac{\alpha_s^2 M_{\eta_Q}|R^{(l)}_{nl}(r)|^2}{3{m_Q}^3}\left[1+4.8\left(\frac{\alpha_S}{\pi}\right)\right], \tag{12}$$

$$\Gamma_{\rm gg}(\chi_{Q_0}) = \frac{3\alpha_s^2 M_{\chi_{Qc0}} |R^{(l)}_{nl}(r)|^2}{{m_Q}^5}\left[1+8.77\left(\frac{\alpha_{\rm S}}{\pi}\right)\right], \quad (13)$$

$$\Gamma_{\rm gg}(\chi_{Q_2}) = \frac{4}{15}\frac{3\alpha_s^2 M_{\chi_{Qc2}} |R^{(l)}_{nl}(r)|^2}{{m_Q}^5}\left[1-4.827\left(\frac{\alpha_{\rm S}}{\pi}\right)\right]. \quad (14)$$

Here, $\alpha = 1/137$ is the electromagnetic coupling constant and e_Q corresponds to the charge content of the $Q\bar{Q}$ meson in terms of the electron charge. For $c\bar{c}$ meson, $e_Q = 2/3$ and $m_Q = m_c$. Within the potential confinement scheme, we consider the constituent quark mass m_c which appears in Eqs.(9–14) as the effective mass of the quark within the bound state of the charmonium system as defined by [49, 50]:

$$m_c^{\rm eff} = m_c\left(1+\frac{\langle E_{\rm bind}\rangle_{nl}}{m_c+m_{\bar{c}}}\right). \quad (15)$$

3.2 Using NRQCD formalism

The new role of the heavy flavour studies as the testing ground for the non-perturbative aspects of QCD demands an extension of earlier phenomenological potential model studies on quarkonium masses to their predictions of decay widths with the non-perturbative approaches like NRQCD. It is expected that the NRQCD formalism has all the corrective contributions for the right predictions of the decay rates. The decay rates of the heavy-quarkonium states into photons and pairs of leptons are among the earliest applications of perturbative quantum chromodynamics (QCD)[43, 51]. In NRQCD formalism decay rates are factorized into short and long distance parts. The short-distance factor is related to the annihilation rate of the heavy quark and antiquark and this part is calculated in terms of the running coupling constant $\alpha_s(m_Q)$ of QCD, evaluated at the scale of the heavy-quark m_Q, while the long-distance factor which contains all nonperturbative effects of the QCD is expressed in terms of the meson's nonrelativistic wave function or derivatives of wavefunctions, evaluated at the origin. Our attempt in this section is to study the digamma and di-lepton decay widths based on the NRQCD formalism [20]. NRQCD factorization expressions for the decay widths of quarkonia are given by [41, 52]

$$\begin{aligned}
&\Gamma(^1S_0\to\gamma\gamma) = \frac{F_{\gamma\gamma}(^1S_0)}{m_Q^2}\left|\langle 0|\chi^\dagger\psi|^1S_0\rangle\right|^2 \\
&+\frac{G_{\gamma\gamma}(^1S_0)}{m_Q^4}{\rm Re}\left[\langle {}^1S_0|\psi^\dagger\chi|0\rangle\left\langle 0|\chi^\dagger\left(-\frac{\rm i}{2}\overrightarrow{D}\right)^2\psi|^1S_0\right\rangle\right] \\
&+\frac{H^1_{\gamma\gamma}(^1S_0)}{m_Q^6}\left\langle {}^1S_0|\psi^\dagger\left(-\frac{\rm i}{2}\overrightarrow{D}\right)^2\chi|0\right\rangle\times \\
&\left\langle 0|\chi^\dagger\left(-\frac{\rm i}{2}\overrightarrow{D}\right)^2\psi|^1S_0\right\rangle+\frac{H^2_{\gamma\gamma}(^1S_0)}{m_Q^6}\times \\
&{\rm Re}\left[\langle {}^1S_0|\psi^\dagger\chi|0\rangle\left\langle 0|\chi^\dagger\left(-\frac{\rm i}{2}\overrightarrow{D}\right)^4\psi|^1S_0\right\rangle\right], \quad (16)\\
&\Gamma(^3S_1\to e^+e^-) = \frac{F_{\rm ee}(^3S_1)}{m_Q^2}\left|\langle 0|\chi^\dagger\sigma\psi|^3S_1\rangle\right|^2 \\
&+\frac{G_{\rm ee}(^3S_1)}{m_Q^4}{\rm Re}\left[\langle {}^3S_1|\psi^\dagger\sigma\chi|0\rangle\right. \\
&\left.\left\langle 0|\chi^\dagger\sigma\left(-\frac{\rm i}{2}\overrightarrow{D}\right)^2\psi|^3S_1\right\rangle\right] \\
&+\frac{H^1_{\rm ee}(^1S_0)}{m_Q^6}\left\langle {}^3S_1|\psi^\dagger\sigma\left(-\frac{\rm i}{2}\overrightarrow{D}\right)^2\chi|0\right\rangle\times \\
&\left\langle 0|\chi^\dagger\sigma\left(-\frac{\rm i}{2}\overrightarrow{D}\right)^2\psi|^3S_1\right\rangle+\frac{H^2_{\rm ee}(^1S_0)}{m_Q^6}\times \\
&{\rm Re}\left[\langle {}^3S_1|\psi^\dagger\sigma\chi|0\rangle\left\langle 0|\chi^\dagger\sigma\left(-\frac{\rm i}{2}\overrightarrow{D}\right)^4\psi|^3S_1\right\rangle\right]. \quad (17)
\end{aligned}$$

The short distance coefficients F' and G' of the order of α_s^2 and α_s^3 are given by [52]

$$\begin{aligned}
&F_{\gamma\gamma}(^1S_0) = 2\pi Q^4\alpha^2\left[1+\left(\frac{\pi^2}{4}-5\right)C_F\frac{\alpha_{\rm s}}{\pi}\right] \\
&G_{\gamma\gamma}(^1S_0) = -\frac{8\pi Q^4}{3}\alpha^2 \\
&H^1_{\gamma\gamma}(^1S_0)+H^2_{\gamma\gamma}(^1S_0) = \frac{136\pi}{45}Q^4\alpha^2, \quad (18)\\
&G_{\rm ee}(^3S_1) = -\frac{8\pi Q^2}{9}\alpha^2 \\
&H^1_{\rm ee}(^3S_1)+H^2_{\rm ee}(^3S_1) = \frac{58\pi}{54}Q^2\alpha^2 \\
&F_{\rm ee}(^3S_1) = \frac{2\pi Q^2\alpha^2}{3}\left\{1-4C_F\frac{\alpha_s(m)}{\pi}+\right. \\
&\left.\left[-117.46+0.82n_{\rm f}+\frac{140\pi^2}{27}\ln\left(\frac{2m}{\mu_A}\right)\right]\left(\frac{\alpha_s}{\pi}\right)^2\right\}. \quad (19)
\end{aligned}$$

For the matrix elements that contribute to the decay rates of the S wave states into $\eta_Q \to \gamma\gamma$ and $\psi \to e^+e^-$ through next-to-leading order in v^2, the vacuum-saturation approximation gives [20]

$$\begin{aligned}
&\langle {}^1S_0|\mathcal{O}(^1S_0)|^1S_0\rangle = \left|\langle 0|\chi^\dagger\psi|^1S_0\rangle\right|^2[1+O(v^4\Gamma)] \\
&\langle {}^3S_1|\mathcal{O}(^3S_1)|^3S_1\rangle = \left|\langle 0|\chi^\dagger\sigma\psi|^3S_1\rangle\right|^2[1+O(v^4\Gamma)] \\
&\langle {}^1S_0|\mathcal{P}_1(^1S_0)|^1S_0\rangle = {\rm Re}\left[\langle {}^1S_0|\psi^\dagger\chi|0\rangle\times\right. \\
&\left.\left\langle 0|\chi^\dagger(-\frac{\rm i}{2}\overrightarrow{D})^2\psi|^1S_0\right\rangle\right]+O(v^4\Gamma) \\
&\langle {}^3S_1|\mathcal{P}_1(^3S_1)|^3S_1\rangle = {\rm Re}\left[\langle {}^3S_1|\psi^\dagger\sigma\chi|0\rangle\times\right.
\end{aligned}$$

$$\left\langle 0|\chi^\dagger\times\sigma\left(-\frac{\mathrm{i}}{2}\overrightarrow{D}\right)^2\psi|^3S_1\right\rangle\Bigg]+O(v^4\Gamma)$$

$$\langle^1S_0|\mathcal{Q}_1^1(^1S_0)|^1S_0\rangle=\left\langle 0|\chi^\dagger\left(-\frac{\mathrm{i}}{2}\overrightarrow{D}\right)^2\psi|^1S_0\right\rangle$$

$$\langle^3S_1|\mathcal{Q}_1^1(^3S_1)|^3S_1\rangle=\left\langle 0|\chi^\dagger\sigma\left(-\frac{\mathrm{i}}{2}\overrightarrow{D}\right)^2\psi|^3S_1\right\rangle \quad (20)$$

The vacuum saturation allows the matrix elements of some four fermion operators to be expressed in terms of the regularized wave-function parameters given by [20]:

$$\langle^1S_0|\mathcal{O}(^1S_0)|^1S_0\rangle=\frac{3}{2\pi}|R_P(0)|^2$$

$$\langle^3S_1|\mathcal{O}(^3S_1)|^3S_1\rangle=\frac{3}{2\pi}|R_V(0)|^2$$

$$\langle^1S_0|\mathcal{P}_1(^1S_0)|^1S_0\rangle=-\frac{3}{2\pi}|\overline{R_P^*}\ \overline{\nabla^2R_P}|$$

$$\langle^3S_1|\mathcal{P}_1(^3S_1)|^3S_1\rangle=-\frac{3}{2\pi}|\overline{R_V^*}\ \overline{\nabla^2R_V}|$$

$$\langle^1S_0|\mathcal{Q}_1^1(^1S_0)|^1S_0\rangle=-\sqrt{\frac{3}{2\pi}}\overline{\nabla^2}R_P$$

$$\langle^3S_1|\mathcal{Q}_1^1(^3S_1)|^3S_1\rangle=-\sqrt{\frac{3}{2\pi}}\overline{\nabla^2}R_V \quad (21)$$

The term $\overline{\nabla^2R_{P/V}}$ is the renormalised Laplacian of the radial wave function. We have computed $\overline{\nabla^2R_{P/V}}$ term as given by Ref. [19]. Accordingly,

$$\overline{\nabla^2R_{P/V}}=-\epsilon_{\rm B}R_{P/V}\frac{M_{P/V}}{2},\quad \text{as}\quad r\to0 \quad (22)$$

where $\epsilon_{\rm B}$ is the binding energy and M is the mass of the respective meson state. The binding energy is computed as $\epsilon_{\rm B}=M-(2m_Q)$.

The rate of the decay can be estimated in the extreme-nonrelativistic picture, where the system is described by the wave function for the quark-antiquark pair and depends on their relative position $\vec{r}=\vec{r_{\rm c}}-\vec{r\bar{c}}$. The annihilation takes place at the characteristic distances of order $1/m_{\rm c}$ which are to be viewed as $r\to0$ for a nonrelativistic pair, so that the decay amplitude is proportional to the wave function at the origin. So the right description of a meson state through its radial wave function at the origin and its mass along with other model parameters like $\alpha_{\rm s}$ and the model quark masses become crucial for the computations of the decay rates. In many cases of potential model predictions, the radial wave functions at the origin are found to overestimate the decay rates. In such cases, it is assumed that the decay of $Q\bar{Q}$ does not occur at zero separation but at some finite $Q\bar{Q}$ radial separation. Then arbitrary scaling of the radial wave function at zero separation is done to estimate the decay rates correctly [58].

In the present study, we have calculated decay properties at zero quark separation ($r=0$) as well as at the finite quark separation $r=r_0$. This quark-antiquark distance is considered as the distance at which the inter-quark potential becomes zero. This radial distance r_0 can be considered as the'colour Compton radius', a quantity related to the electromagnetic processes, as referred to by the authors in [41, 58]. We define r_0 by

$$r_0=\frac{N_{\rm c}|e_Q|}{M_{P/V}} \quad (23)$$

of the charmonia state. It is similar to the Compton radius and we call it the color Compton radius of the $\rm c\bar{c}$ systems. Here, N_c is the number of flavors and e_Q is the charge of the quark in terms of the electron charge. However, particularly in the prediction of the leptonic decay widths, considerable improvement has been obtained when it is evaluated at finite distance r_0. The computed di-leptonic and di-gamma decay widths using two formalisms, i.e. with Van Royen-Weisskopf formula and with NRQCD formalism, are listed in Tables 5 and 6 respectively to give a clear comparison. The computed di-gamma widths of the P waves $\rm c\bar{c}$ states are listed in Table 7 while the di-gluon widths of S and P wave $\rm c\bar{c}$ states are listed in Tables 8 and 9 respectively. The computed widths are represented as $\Gamma_{0/0\rm R}(0)$, $\Gamma_{0/0\rm R}(r_0)$ for the di-leptonic and di-gamma decay widths and $\Gamma_{\rm gg/ggR}(0)$, $\Gamma_{\rm gg/ggR}(r_0)$ for the di-gluon decay widths. The quantities, with suffixes carrying R, correspond to the widths with the respective radiative corrections included.

Table 4. Charmonium mass splitting compared to experimental and other predictions (in MeV).

mass difference	present	[57]	[56]	[41]	experiment
$1P$-$1S$ splitting	471	457.3 ± 3.6	455	863.5	457.5 ± 0.3
$1S$ hyperfine	118	$118.1\pm2.1^{-1.5}_{-4.0}$	116.74	174	113.2 ± 0.7
$1P$ spin-orbit	34.11	49.5 ± 2.5	65.88	–	46.6 ± 0.1
$1P$ tensor	20.11	17.3 ± 2.9	13.17	–	16.25 ± 0.22
$2S$-$1S$ splitting	593	–	606	529	606 ± 1

Table 5. Di-leptonic decay widths of charmonium in Van Royen-Weisskopf formula (VRW) as well as NRQCD formalism in keV.

state	VRW formula				NRQCD			Exp
	$\Gamma_0(0)$	$\Gamma_{0\mathrm{R}}(0)$	$\Gamma_0(r_0)$	$\Gamma_{0\mathrm{R}}(r_0)$	$\Gamma_0(0)$	$\Gamma_{0\mathrm{R}}(0)$	$\Gamma_{0\mathrm{R}}(r_0)$	
J/ψ(1S)	9.22	4.61	5.01	2.50	7.280	7.190	6.730	5.55±0.14
others	4.95 [56]				4.698 [15]			
	1.85 [59]				10.294 [58]			
					2.809 [60]			
					5.470 [61]			
					2.94 [62]			
ψ(2S)	6.87	3.43	2.33	1.16	3.397	3.354	3.250	2.35±0.04
others	2.33 [56]				2.14 [61]			
	0.89 [59]				1.22 [62]			
ψ(3S)	5.89	3.04	1.64	0.820	3.089	3.250	0.82	0.86±0.004
others	1.63 [56]				0.796 [61]			
	0.98 [59]				0.76 [62]			

Table 6. Di-gamma decay widths of charmonia states in Van Royen-Weisskopf formula (VRW) as well as NRQCD formalism in keV.

state	VRW formula				NRQCD			Exp*
	$\Gamma_0(0)$	$\Gamma_{0\mathrm{R}}(0)$	$\Gamma_0(r_0)$	$\Gamma_{0\mathrm{R}}(r_0)$	$\Gamma_0(0)$	$\Gamma_{0\mathrm{R}}(0)$	$\Gamma_{0\mathrm{R}}(r_0)$	
1^1S_0	11.49	7.853	4.022	2.747	18.19	13.30	6.73	5.055±0.411[6]
others	10.37 [56]				10.691 [15]			
	8.5 [63]				17.447 [58]			
					6.561 [60]			
2^1S_0	8.873	6.061	1.869	1.276	14.01	10.34	3.27	2.147±1.580 [6]
others	3.349 [56]				1.8 [8]			
	2.4 [63]				4.44±0.48 [11]			
					3.5–4.5 [46]			
3^1S_0	7.458	5.098	0.9780	0.6679	13.93	8.81	1.94	–
others	1.900 [56]				1.21 [54]			

Table 7. Di-gamma decay widths of P waves charmonia states using m_{eff} in keV.

state	1^3P_0	1^3P_2	2^3P_0	2^3P_2
$\Gamma_0(0)$	9.964	1.358	5.46	1.48
$\Gamma_{0\mathrm{R}}(0)$	5.065	0.68	2.97	0.74
$\Gamma_0(r_0)$	8.789	1.197	4.02	1.09
$\Gamma_{0\mathrm{R}}$	4.468	0.599	1.04	0.54
others	2.341±0.189 [6]	0.528±0.404 [6]	1.7 [63]	0.23 [63]
	2.5 [63]	0.31 [63]		
	2.36±0.35 [64]	$0.346^{+0.009}_{0.011}$ [64]		
	5.0 [46]	0.70 [46]		
	6.38 [65]	0.57 [65]		
	3.96 [66]	0.743 [66]		

*The di-gamma decay widths are estimated using the values of branching fraction and full decay width given in PDG[2014]

Table 8. Di-gluon decay for nS states for charmonia states in MeV.

state	decay width	present	others
	$\Gamma^{m}_{\rm gg}(0)$	38.47	32.20 [44]
	$\Gamma^{m}_{\rm ggR}(0)$	55.80	10.70 [67]
	$\Gamma^{\rm meff}_{\rm gg}(0)$	22.37	19.60 [11]
1^1S_0	$\Gamma^{\rm meff}_{\rm ggR}(0)$	32.45	23.03 [65]
	$\Gamma^{m}_{\rm gg}(r_0)$	12.70	9.010 [68]
	$\Gamma^{m}_{\rm ggR}(r_0)$	18.42	26.7 ± 3.0 [6]
	$\Gamma^{\rm meff}_{\rm gg}(r_0)$	7.38	
	$\Gamma^{\rm meff}_{\rm ggR}(r_0)$	10.71	
	$\Gamma^{m}_{\rm gg}(0)$	47.47	8.10 [67]
	$\Gamma^{m}_{\rm ggR}(0)$	38.86	12.1 [11]
	$\Gamma^{\rm meff}_{\rm gg}(0)$	16.74	14.7 ± 0.7 [6]
2^1S_0	$\Gamma^{\rm meff}_{\rm ggR}(0)$	24.29	
	$\Gamma^{m}_{\rm gg}(r_0)$	10.02	
	$\Gamma^{m}_{\rm ggR}(r_0)$	14.54	
	$\Gamma^{\rm meff}_{\rm gg}(r_0)$	3.558	
	$\Gamma^{\rm meff}_{\rm ggR}(r_0)$	5.133	
	$\Gamma^{m}_{\rm gg}(0)$	56.02	
	$\Gamma^{m}_{\rm ggR}(0)$	81.26	
	$\Gamma^{\rm meff}_{\rm gg}(0)$	14.03	
3^1S_0	$\Gamma^{\rm meff}_{\rm ggR}(0)$	20.36	
	$\Gamma^{m}_{\rm gg}(r_0)$	7.170	
	$\Gamma^{m}_{\rm ggR}(r_0)$	10.40	
	$\Gamma^{\rm meff}_{\rm gg}(r_0)$	1.796	
	$\Gamma^{\rm meff}_{\rm ggR}(r_0)$	2.606	

4 Results and discussion

Using the predicted masses and radial wave functions at the origin as well as at finite quark-antiquark separation, the di-gamma and di-leptonic decays of charmonia are computed using the conventional Van Royen-Weisskopf non-relativistic formula as well as using NRQCD formalism.

Apart from this, di-gloun decays of charmonia are also studied using conventional the Van Royen-Weisskopf formula. The overall agreement of the calculated mass spectra with the experiment [6] and lattice results [53] is impressive. The present study also shows us the importance of the quark mass parameters and the state dependence on the potential strength for the study of the spectral properties of $c\bar{c}$ mesons. This study is also an attempt towards a quantitative understanding of the importance of radiative corrections for the decay widths of the heavy flavour quarkonia. The results for mass spectra of S wave states are shown in Table 1 while those for P and D waves with spin-orbit and tensor contributions are shown in Tables 2 and 3 respectively. These results are in good agreement with the available experimental values with just about 1.09% variations, while comparison with those of the lattice QCD predictions show 1.46% variation.

Table 9. Di-gluon decay for P waves for charmonia states in MeV.

state	decay width	present	others
	$\Gamma^{m}_{\rm gg}(0)$	47.88	10.46 [44]
	$\Gamma^{m}_{\rm ggR}(0)$	81.18	13.44 [65]
	$\Gamma^{\rm meff}_{\rm gg}(0)$	9.45	12.5 ± 3.2 [69]
1^1P_0	$\Gamma^{\rm meff}_{\rm ggR}(0)$	17.21	10.4 ± 0.7 [6]
	$\Gamma^{m}_{\rm gg}(r_0)$	41.07	
	$\Gamma^{m}_{\rm ggR}(r_0)$	74.77	
	$\Gamma^{\rm meff}_{\rm gg}(r_0)$	8.271	
	$\Gamma^{\rm meff}_{\rm ggR}(r_0)$	15.05	
	$\Gamma^{m}_{\rm gg}(0)$	14.02	1.169 [44]
	$\Gamma^{m}_{\rm ggR}(0)$	7.82	1.2 [65]
	$\Gamma^{\rm meff}_{\rm gg}(0)$	2.81	1.72 [67]
1^3P_2	$\Gamma^{\rm meff}_{\rm ggR}(0)$	1.54	2.03 ± 0.12 [6]
	$\Gamma^{m}_{\rm gg}(r_0)$	12.62	
	$\Gamma^{m}_{\rm ggR}(r_0)$	6.922	
	$\Gamma^{\rm meff}_{\rm gg}(r_0)$	2.465	
	$\Gamma^{\rm meff}_{\rm ggR}(r_0)$	1.351	
	$\Gamma^{m}_{\rm gg}(0)$	103.2	9.61 [45]
	$\Gamma^{m}_{\rm ggR}(0)$	187.9	
	$\Gamma^{\rm meff}_{\rm gg}(0)$	10.09	
2^1P_0	$\Gamma^{\rm meff}_{\rm ggR}(0)$	18.38	
	$\Gamma^{m}_{\rm gg}(r_0)$	27.69	
	$\Gamma^{m}_{\rm ggR}(r_0)$	15.18	
	$\Gamma^{\rm meff}_{\rm gg}(r_0)$	2.70	
	$\Gamma^{\rm meff}_{\rm ggR}(r_0)$	1.48	
	$\Gamma^{m}_{\rm gg}(0)$	75.06	
	$\Gamma^{m}_{\rm ggR}(0)$	136.6	
	$\Gamma^{\rm meff}_{\rm gg}(0)$	7.34	
2^3P_2	$\Gamma^{\rm meff}_{\rm ggR}(0)$	13.37	
	$\Gamma^{m}_{\rm gg}(r_0)$	20.39	
	$\Gamma^{m}_{\rm ggR}(r_0)$	11.18	
	$\Gamma^{\rm meff}_{\rm gg}(r_0)$	1.99	
	$\Gamma^{\rm meff}_{\rm ggR}(r_0)$	1.09	

The precise experimental measurements of the masses of charmonia states provide a real test for the choice of the hyperfine and the fine structure interactions adopted in the study of charmonia spectroscopy. Hyperfine splitting provides a direct measure of the strength of the spin-spin chromomagnetic interaction. Recently, charmonium mass splittings in three flavor lattice QCD has been studied by the Fermilab Lattice and MILC collaborations [57]. In Table 4, we have compared our results for the mass splittings with the lattice results as well as with the respective experimental results and also with other potential model predictions. Both spin-orbit and tensor terms test the strength of the chromoelectric interaction. The tensor term is in good agreement with lattice as well

as experimental results while the spin orbit term is off from the experimental as well as lattice results. The spin-averaged $1P$-$1S$ splitting tests the central part of the potential. The splitting of the spin-averaged $2S$ and $1S$ levels also tests the central part of the quarkonium effective potential. One of the important features of the present potential model is that the nature of the quark-antiquark potential exactly mimics the Cornell-like potential, as seen from Fig. 1. Another important feature of this study is that the decay of the charmonium system occurs at a finite range of its separation provided by the color Compton radius. This suggests that various processes of quark-antiquark annihilation occur at finite radial separation.

The di-leptonic decay widths computed at finite radial separation defined through the color Compton radius are found to be in better agreement with the experimental values for most of the states. The leptonic decay widths $\Gamma_{0\mathrm{R}}$ for $1S$ state and $3S$ at finite distance r_0 with the inclusion of radiative correction are found to be in good agreement with the experimental data while for $2S$ state, the decay width Γ_0 matches well with experimental results without inclusion of radiative corrections.

For the $1S$ and $2S$ states, the computed di-gamma widths $\Gamma_0(r_0)$ at finite quark-antiquark separation without radiative correction are in good agreement with the experimental results while for the $3S$ state the experimental data are not available. The results for the χ_{c_0} state are slightly off from the experimental results but are in agreement with the other model predictions [46, 63]. The di-gamma decay width $\Gamma_{0\mathrm{R}}(r_0)$ predicted for the 1^3P_2 state at finite quark-antiquark separation matches well with the experimental result, while the decay width $\Gamma_{0\mathrm{R}}(0)$ agrees well with the experimental result. Though we predict the di-gamma decay widths of $2P$ states, they have not been measured experimentally, so we have compared our results with the other available theoretical predictions.

The di-gluon decay widths predicted for the $c\bar{c}$ system are all in good agreement with available experimental data as well as other model predictions. It is observed that the di-gluon decay widths of $1S$ and $2S$ states of $c\bar{c}$ without radiative corrections and with binding energy effects are consistent with experimental values when evaluated at the origin. On the other side the di-gluon decay widths of $1S$ and $2S$ states of $c\bar{c}$ with radiative corrections and without inclusion of the binding energy effects are consistent with experimental values when evaluated at some finite distance.

The predicted di-gluon decay width of the χ_{c0} state with the inclusion of binding energy effects and without radiative corrections agrees well with the experimental values when it is evaluated at the origin and finite distance r_0. For the χ_{c2} state the decay width without inclusion of binding energy effects and without radiative correction is in agreement with the experimental value when it is evaluated at the origin. In the case of the di-leptonic decay width, the RMS variation when it is evaluated at finite quark-antiquark separation r_0, without and with inclusion of radiative corrections is 0.50 and 1.80 respectively, which is less than the RMS variation when calculated at the origin, so the leptonic decay occurs at finite quark-antiquark separation r_0.

The RMS variation in di-gamma decay when evaluated at the origin, without and with inclusion of radiative corrections is 4.89 and 2.60 respectively. This RMS variation in di-gamma decay width becomes less when it is evaluated at finite quark-antiquark separation r_0 i.e. it is 3.19 and 1.56, without and with inclusion of radiative corrections respectively. So in the case of di-gamma decay , finite separation as well as radiative corrections are both important. There is a large RMS variation in the di-gluon decay width when it is calculated with quark mass m, but this variation decreases when it is evaluated with the inclusion of binding energy effects (i.e. with effective quark mass). In the case of the di-gluon decay width, the RMS variation is 2.46 and 6.55 when evaluated at zero quark-antiquark separation without and with inclusion of radiative corrections, but the RMS variation in di-gluon decay width is 11.2 and 9.61 when evaluated at r_0 without and with inclusion of radiative corrections, so in the case of di-gluon decay finite separation is found not to be important. We predict the di-gluon decay width of 3S and 2P states of charmonia and we look forward to seeing the experimental support in favour of our predictions.

In the NRQCD formalism the di-leptonic and di-gamma decay widths have been computed by using the radial wavefunctions and their derivatives at the origin as well at some finite distance seperation. The predicted di-leptonic decay widths evaluated at the origin with and without inclusion of radiative corrections are found to be overestimated while those which are evaluated at some finite separation are found to be in better agreement with the experimental data as well as other theoretical predictions. The same trend is seen in the case of the di-gamma decay widths. With the NRQCD formalism, the RMS variations in the di-leptonic and di-gamma decay are 0.29 and 0.83 respectively when evaluated at finite radial separation. It can be concluded that the NRQCD formalism has most of the corrective contributions required for most of the potential models for the right predictions of the decay rates. Finally, we believe that future high luminosity experiments will be able to shed more light on the understanding of the quark-antiquark interaction.

References

1 G. Bonvicini et al (CLEO Collaboration), Phys. Rev. D, **81**: 031104 (2010)
2 K. M. Ecklund et al (CLEO Collaboration), Phys. Rev. D, **78**: 091501 (2008)
3 B. Auger et al (BABAR Collaboration), Phys. Rev. Lett., **103**: 161801 (2009)
4 N Brambilla et al, 2011 Eur. Phys. J. C, **71**: 1534
5 K. Nakamura (Particle Data Group), 2010 J. Phys. G: Nucl. Part. Phys., **37**: 075021
6 K. A. Olive et al (Particle Data Group), Chinese Physics C, **38**: (9) 090001 (2014)
7 M. R. Ahmady and R. R. Mendel, Phys. Rev. D, **51**: 141 (1995)
8 D. Ebert, R. N. Faustov, and V. O. Galkin, Mod. Phys. Lett. A, **18**: 601 (2003)
9 C. W. Hwang and Z. T. Wei, J. Phys. G, **34**: 687 (2007)
10 H. W. Huang, J. H. Liu, J. Tang, and K. T. Chao, Phys. Rev. D, **56**: 368 (1997)
11 C. S. Kim, T. Lee, and G. L. Wang, Phys. Lett. B, **606**: 323 (2005)
12 J. P. Lansberg and T. N. Pham, Phys. Rev. D, **74**: 034001 (2006); **75**: 017501 (2007)
13 J. J. Dudek and R. G. Edwards, Phys. Rev. Lett., **97**: 172001 (2006)
14 W. Buchmuller, S.H.H. Tye, Phys. Rev. D, **24**: 132 (1981)
15 A. Martin, Phys. Lett. B, **93**: 338 (1980)
16 C. Quigg and J.L. Rosner, Phys. Lett. B, **71**: 153 (1977)
17 A. K. Rai, J.N. Pandya, and P. C. Vinodkumar, J. Phys. G: Nucl. Part. Phys., **31**: 1453 (2005)
18 S. S. Gershtein, V.V. Kiselev, A.K. Likhoded, and A. V. Tkabladze, Phys. Rev. D, **51**: 3613 (1995)
19 H. Khan and P. Hoodbhoy, Phys. Rev. D, **53**: 2534 (1996)
20 G. T. Bodwin, E. Braaten, and G. P. Lepage, Phys. Rev. D, **51**: 1125 (1995); **55**: 5853 (1997)(E)
21 G. T. Bodwin, D. Kang, and J. Lee, Phys. Rev. D, **74**: 014014(2006)
22 G. T. Bodwin, H.S. Chang, D. Kang, J. Lee, and Chaehyun Yu, Phys. Rev. D, **77**: 094017 (2008)
23 N.N. Singh et al, Phys. Rev. D, **38**: 1454 (1988); S. Chakrabarty et al, Prog. Part. Nucl. Phys., **22**: 143180 (1989)
24 A. Mittal et al, Phys. Rev. Lett., **57**: 290 (1986); K. K. Gupta et al, Phys. Rev. D, **42**: 1604 (1990); A. Sharma et al, Phys. Rev. D, **50**: 454 (1994)
25 S.Bhatnagar, and S-Y.Li, J. Phys. G, **32**: 949 (2006)
26 S. Bhatnagar, J. Mahecha, and Y. Mengesha, Phys. Rev D, **90**: 014034 (2014)
27 R. Alkofer, P. Watson, and H. Weigel, Phys. Rev. D, **65**: 094026 (2002)
28 R. Alkofer and L. W. Smekel, Phys. Rep., **353**: 281 (2001)
29 G. Cvetic, C. S. Kim, G.-Li Wang, and W. Namgung, Phys. Lett. B, **596**: 84 (2004)
30 A. N. Mitra and B. M. Sodermark, Nucl. Phys. A, **695**: 328 (2001)
31 T. Barnes, S. Godfrey, and E.S. Swanson, Phys. Rev. D, **72**: 054026(2005)
32 Olga Lakhina and Eric S. Swanson, Phys. Rev D, **74**: 014012 (2006), arXiv:hep-ph/0603164
33 M.B. Voloshin, Prog. Part. Nucl. Phys., **61**: 455 (2008), arXiv:0711.4556 [hep-ph]
34 E. Eichten, S. Godfrey, and H. Mahlke, J.L. Rosner, Rev. Mod. Phys., **80**: 1161(2008)
35 W. Lucha and F. Shoberl, Int. J. Mod. Phys. C, **10**: (1999), arXiv:hep-ph/9811453
36 L. Landau, Phys. Abstracts A, **52**: 125(1949)
37 C. N. Yang, Phys. Rev., **77**: 242 (1950)
38 Kwong Waikwok et al, Phys. Rev. D, **37**: 3210 (1988)
39 Arpit Parmar, Bhavin Patel, and P. C. Vinodkumar, Nuclear Physics A, **848**: 299-316 (2010)
40 Patel Bhavin, et al, J. Phys. G: Nucl. Part. Phys., **36**: 035003 (2009)
41 Rai A K, Patel B, and Vinodkumar P C, Phys. Rev. C, **78**: 055202(2008)
42 Han-Wen Huang and Kuang-Ta Chao, Phys. Rev. D, **54**: 6850 (1996); Han-Wen Huang and Kuang-Ta Chao, Phys. Rev. D, **56**: 182(1996)
43 R. Barbieri, R. Gatto, and R. Kogerler, Phys. Lett. B, **60**: 183 (1976)
44 A. Petrelli, M. Cacciari, M. Greco, F. Maltoni, and M.L. Mangano, Nucl. Phys. B, **514**: 245 (1998)
45 Wang G L, Phys. Lett. B, **653**; 206 (2007)
46 J. P. Lansberg, and T. N. Pham, Phys. Rev. D, **79**: 094016 (2009), arXiv:0903.1562 [hep-ph]
47 R. Barbieri, M. Caffo, R. Gatto, and E. Remiddi, Nucl. Phys. B, **192**: 61(1981)
48 M. Mangano and A. Petrelli, Phys. Lett. B, **352**: 445 (1995)
49 Bhavin Patel et al, J. Phy. G.: Nucl. Part. Phys., **35**: 065001 (2008)
50 P C Vinodkumar and Bhavin Patel, Chinese Phys. C, **34**: 1411(2010)
51 Appelquist T and Politzer H D, Phys. Rev. Lett., **34**: 43 (1975)
52 Bodwin G T and Petrelli A, Phys. Rev. D, **66**: 094011 (2002)
53 Bali G S, Schiling K, and Wachter A, Phys. Rev. D, **56**: 2566
54 Lakhina O and Swanson E S, Phys. Rev. D, **74**: 014012 (2006)
55 Okamoto M et al, Phys. Rev. D, **65**: 094508 (2002)
56 M. Shah, A. Parmar, and P. C. Vinodkumar, Phys. Rev. D, **86**: 034015 (2012)
57 Daniel Mohler et al, Fermilab Lattice and MILC Collaborations, arXiv:hep-lat/1412.1057v1
58 E. Eichten, K. Gottfried, T. Kinoshita, K. D. Lane, and T. M.Yan, Phys. Rev. D, **17**: 3090 (1978)
59 Stanley F. Radford, and Wayne W. Repko, Phys. Rev. D, **75**: 074031 (2007)
60 Buchmuller and Tye, Phys. Rev. D, **24**: 132 (1981)
61 Vinodkumar P C, Pandya J N, Bannur V M, and Khadkikar S B, Eur. Phys.J. A, 4: 83 (1999)
62 Gonzalez P, Valcarce A, Garcilazo H, and Vijande J, Phys. Rev. D, **68**: 034007 (2003)
63 Bai-Qing Li and Kuang-Ta Chao, Phys. Rev. D, **79**: 094004 (2009)
64 Chien-Wen Hwang and Rurng-Sheng Guo, Phy. Rev. D, **82**: 034021 (2010)
65 S N Gupta et al, Phy. Rev. D, **54**: 2075 (1996)
66 H. W. Crater, C. Y. Wong, and P. VanAlstine, Phys. Rev. D, **74**: 054028 (2006)
67 James T L et al, arXiv:hep-ph/0901.3917
68 M. G. Olsson, A. D. Martin, and A.W. Peacock, Phys. Rev. D, **31**: 81 (1985)
69 Huang H W et al, Phys. Rev. D, **54**: 2123 (1996)